

VARIABILITY OF THE ROTLIEGEND SANDSTONES IN THE POLISH PART OF THE SOUTHERN PERMIAN BASIN – PERMEABILITY AND POROSITY RELATIONSHIPS

Jadwiga JARZYNA, Edyta PUSKARCZYK, Maria BAŁA & Bartosz PAPIERNIK

*AGH University of Science and Technology, Faculty of Geology, Geophysics and Environmental Protection,
al. Mickiewicza 30, 30-059 Kraków, Poland, e-mails: jarzyna@uci.agh.edu.pl, puskarczyk@geol.agh.edu.pl,
bala@geol.agh.edu.pl, papiern@geol.agh.edu.pl*

Jarzyna, J., Puskarczyk, E., Bała, M. & Papiernik, B., 2009. Variability of the Rotliegend sandstones in the Polish part of the Southern Permian Basin – permeability and porosity relationships. *Annales Societatis Geologorum Poloniae*, 79: 13–26.

Abstract: The Flow Zone Index, FZI, applied to order relations between the effective porosity and permeability of the Rotliegend sandstones in the Polish part of the Southern Permian Basin turns out to be a useful and effective factor to evaluate ability of media flow in a rock formation. A dataset of over 2000 samples from 78 wells was analysed. Based only on porosity and permeability, FZI includes all non-parameterized features of rocks as tortuosity and diameters of porous channels, volume of trapped parts of capillary roads, specific surface of pore space, and others. When FZI increases, the ability of fluid to move through the porous space increases. In most cases, the Rotliegend sandstones reveal FZI in the range of 0.5–2.0. The highest FZI, ca. 100, is related to fractured part of the studied formation. The combination of FZI and facies information from several wells in the study area (over 1200 samples) showed a good correlation. On the basis of FZI we can divide a set of samples of the Rotliegend sandstone into groups of defined fluid flow abilities and relate them to facies. Also, we show the way of estimation of the reliable values of permeability in full geological log of a borehole on the basis of FZI, and the total porosity determined from well logging interpretation.

Key words: Rotliegend sandstones, porosity, permeability, Flow Zone Index, FZI, facies.

Manuscript received 25 September 2008, accepted 8 April 2009

INTRODUCTION

A dependence between permeability and porosity has been the subject of discussion in the petrophysical literature for many years. A widely used log-linear relationship between the two mentioned reservoir parameters does not correctly comprise the whole information delivered by such factors, as: the size and shape of mineral grains, orientation of grains, packing of grains in the rock mass, degree of sorting, and other factors that strongly influence permeability. Using the simple log-linear relationship for rocks with varied lithology, one can parameterize neither the shape of the pore space, nor the pore tortuosity and the size of throats in the pore space. The relation between porosity and permeability comprises also information on diagenesis and mechanical processes during transportation, deposition and compaction, and deformation of sedimentary material. However, those relations have not yet been mathematically described. The application of the Flow Zone Index (FZI) for describing rock medium capability to fluid transport improves the accuracy of evaluating reservoir parameters. Applying the FZI, a given deposit can be divided into smaller

parts showing similar hydraulic properties. Also, more accurate relationships between porosity and permeability can be obtained for small units (Salem, 1993; Prasad, 2000; Tiab & Donaldson, 2000; Mohammed & Corbett, 2003; Bała *et al.*, 2003; Bała & Jarzyna, 2004; Attia, 2005; Jarzyna & Bała, 2005).

The objective of the paper is to evaluate proper permeability vs. porosity relations for the Rotliegend sandstones of various facies based on laboratory measurements for samples from selected boreholes in the Polish part of the Southern Permian Basin. A method of continuous determination of permeability in a vertical section of borehole according to FZI division using porosity from well log interpretation is also given here.

GEOLOGICAL SETTING

The Rotliegend formations occurring in Central and Western Europe in the Southern Permian Basin were deposited in a continental basin displaying features of a tectonic half-graben (Pokorski, 1998). The shape of the basin and

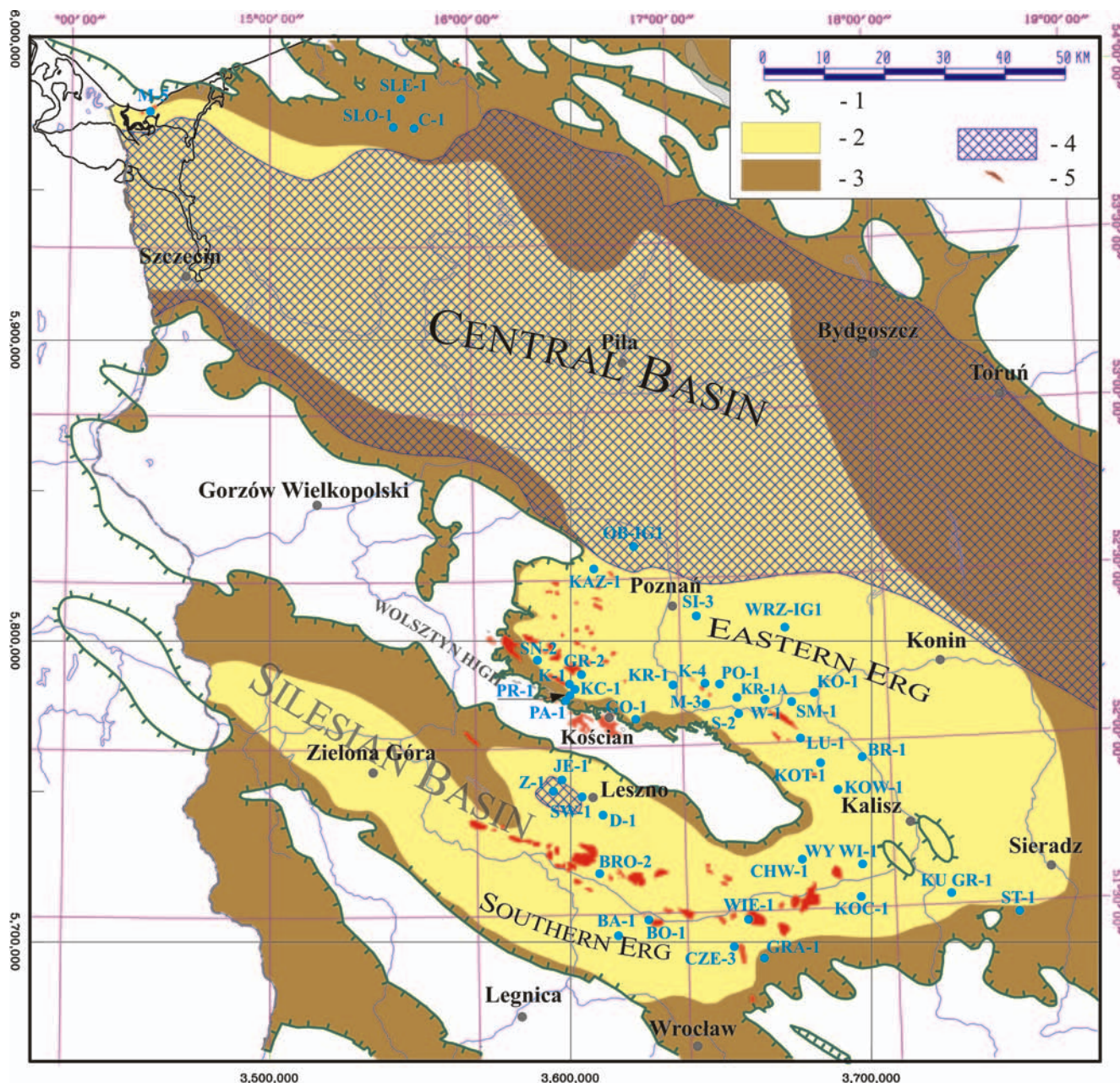


Fig. 1. Location map of the Rotliegend reservoirs and facies distribution: 1 – extent of the Rotliegend deposits; 2 – aeolian facies (reservoir); 3 – fluvial facies (reservoir); 4 – non reservoir playa facies; 5 – gas fields

palaeoclimate conditions caused thickness and facies distribution in the basin to be markedly asymmetric (Kiersnowski, 1998). The maximum thickness of the Rotliegend sediments, exceeding 1,200 m, is observed in the zone of maximal subsidence extending along the NE edge of the basin.

The basin fill consists of sandy-muddy-shaly sediments, which belong to three main desert depositional systems. The deposits of seasonal rivers (alluvial fans and fluvial channels) form the fluvial system. The deposits of dune and interdune environments form the aeolian system. The largest thickness is noted in the central part of the basin dominated by shaly-sandy lithofacies and marginal playa facies of the lacustrine system.

A number of palaeogeographic units are distinguished in the Polish part of the Rotliegend basin (Pokorski, 1981; Karnkowski, 1987). The largest unit is the Central Basin (Pokorski, 1997). Playa and fluvial deposits prevail in the northeastern part of the Central Basin. Aeolian deposits form there sparse intercalations of small thickness, there. In the southeastern part of the Central Basin, fluvial deposits dominate. Aeolian and playa rocks constitute here minor admixtures. Along the southern margin of the Central Basin, aeolian sandstones build the dune area referred to as the Eastern Erg (Kiersnowski, 1997; Kiersnowski & Buniak, 2006). Another palaeogeographic unit important to petroleum prospecting is the Silesian Basin that extends in the southern part of the Fore-Sudetic Homocline. In this broad

Table 1

Relationships between permeability and porosity: regression equations and correlation coefficients for selected wells in the study area

Well	Linear regression equation, $\log K = a\Phi_{\text{eff}} + b$		Correlation coefficient R	Number of sandstone samples in analysis/Total number of samples
	a	b		
B-1	0.12	1.65	0.84	40/66
C-1	0.24	2.24	0.82	87/204
CZ-IG2	0.10	0.79	0.59	63/213
KA-1	0.21	2.26	0.76	51/90
KO-1	0.10	1.05	0.67	92/126
M-5	0.22	-2.22	0.89	202/272
S-2	0.14	-0.60	0.68	71/80
SO-2	0.11	-2.14	0.70	51/74
W-1	0.06	0.64	0.23	317/349
Z-1	0.24	-2.29	0.92	95/104
ZA-1	0.10	-0.42	0.49	89/99

zone, fluvial and aeolian sedimentary systems co-exist. The Wolsztyn High separates the Central Basin and the Silesian Basin. It is surrounded by a narrow belt of fluvial facies, which interfinger with the aeolian sandstones.

The presented investigations concentrate mainly on potential sandstone reservoirs, representing a variety of facies of the above mentioned depositional systems. The quality of the data and necessary clarity of the text result in some terminological simplifications. Deposits belonging to the aeolian depositional system comprise interdune and dune sandstones. In the text they are referred to as aeolian facies. In the collected data set, fluvial system deposits are represented mainly by fluvial channel sandstones, mudstones and conglomerates, and to some extent by alluvial sheet-flood facies. All these sediments are gathered in the fluvial/alluvial fan facies group. Lacustrine sandstones are referred to as playa facies.

The locations of studied wells in terms of the dominant facies are presented in Figure 1. It can be seen that close to the Wolsztyn High the Rotliegend sediments are fluvial sandstones. At a short distance both to the south and to the north they are replaced by aeolian sandstones. However, regardless of facies domination, intercalations of fluvial deposits of considerable thickness can occur in aeolian sediments. Similarly, in areas depicted in Figure 1 as dominated by fluvial sediments some aeolian strata can exist. In the central part of the Rotliegend Basin, regardless of dominant playa facies, sediments belonging to other distinguished depositional systems are present. For example, in well OB IG-1 we observe aeolian facies and playa facies in similar proportions. In the northwestern part of the study area, where well C-5 is located in the area of domination of aeolian sediments and wells SLE-1, SLO-1 and well C-1 are lo-

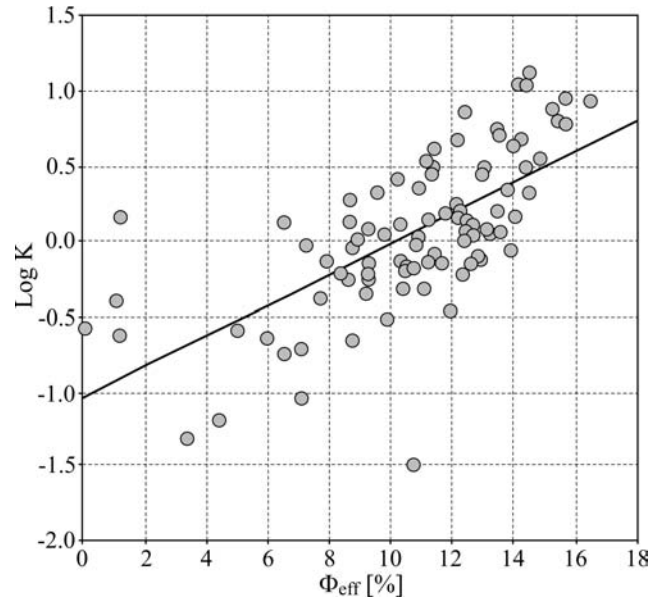


Fig. 2. Dispersion plot $\log K$ vs. Φ_{eff} of the dataset from well KO-1

cated in the zone of prevailing fluvial sediments, some playa sediments are also distinguished.

POROSITY AND PERMEABILITY FROM LABORATORY MEASUREMENTS

The study area included 78 wells, which pierced or only reached the Rotliegend rocks in the Polish part of Southern Permian Basin (Fig. 1). Wells are analysed individually and in groups, concentrated around the towns of Leszno, Kościan, Kalisz, Sieradz, Piła, and Międzyzdroje. From each group, several wells with considerable amount of data with identified lithology and recognized facies are selected to the detailed analysis.

Three main rock types: sandstones, mudstones and shales were drilled through in the Rotliegend deposits. The lithology was determined based on macroscopic core descriptions. At the first step, correlations between absolute permeability, K , and effective porosity, Φ_{eff} , of sandstones were calculated for individual wells. Correlation coefficients, R , changed over a wide range and slopes and intercepts in the regression equations varied significantly (Table 1). This attests to large variability of the analysed material. For several wells high values of R are obtained. These point to a close relationship between absolute permeability and effective porosity due to homogeneous lithofacies data and a sufficient number of samples that assured the statistical correctness (Górecki *et al.*, 2008).

Exemplary dispersion plots $\log K$ vs. Φ_{eff} for data from well KO-1 show good correlation proven by high correlation coefficient equal to 0.68 (Fig. 2). Frequency histograms for porosity and permeability are made for the same datasets (Fig. 3). The Gaussian distribution for porosity and log-normal distribution for permeability are also presented against the background of the histograms.

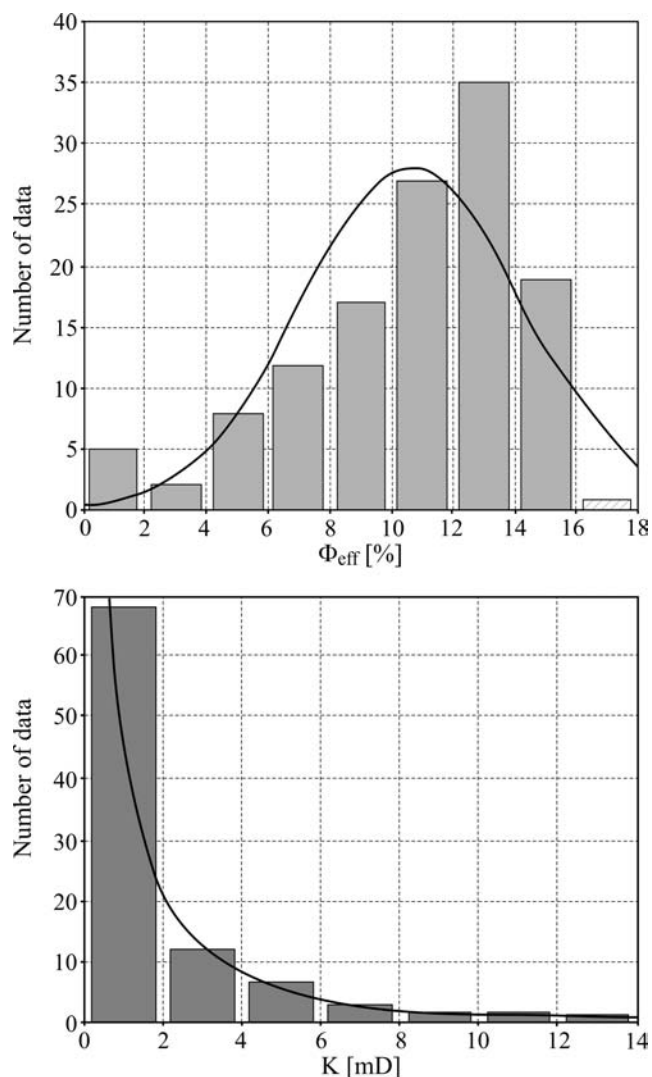


Fig. 3. Frequency histograms of effective porosity and absolute permeability for well KO-1

In the presented example, the porosity distribution is not fully normal due to observed concentration of high values in the range of 12–14% (Fig. 3). The distribution of permeability is almost log-normal (Fig. 3). Low values of permeability dominate in all studied well datasets. The lowest permeability are observed in fluvial facies area. Higher porosity and permeability prevail for samples from wells (among others KO-1) situated in aeolian facies area. Occurrence of illite in cements of sandstone samples (for example in KO-1) and both kaolinite and chlorite in others is also the reason of a difference in porosity and permeability distribution. A maximum burial depth is another factor influencing both porosity and permeability on a basin wide scale. This parameter is especially high in the north-eastern region (Biernacka *et al.*, 2006; Papiernik *et al.*, 2007; Górecki *et al.*, 2008). Similar images of porosity and permeability distributions are observed for the rest of analysed wells. Although a great number of porosity-permeability pairs from the Rotliegend sandstones were analysed, the relations between absolute permeability and effective porosity calculated individually for data from each well cannot be the basis to predict K based on Φ_{eff} .



Fig. 4. Location map of regions A, B, C and D against the background of the map of Poland

GROUPING OF WELLS

The studied wells are grouped according to their geographical location and depth to the top of the Rotliegend sediments. The division is also related with the facies development (Poszytek, 2007). Four main regions: A, B, C, and D were separated (Fig. 4, Table 2).

Correlation analysis is made for permeability vs. porosity for regions A, C and D and for groups B1 – B6 in region B. The results are listed in Table 3. A high correlation coefficient, $R = 0.72$, is obtained for region A. For groups of region B, correlation coefficients only slightly improve as compared to the results for single wells. This is probably due to large variability of petrophysical parameters of the Rotliegend sandstones in those groups. In all regions, porosity varies from 0 or almost 0 up to 26.14 per cent, while permeability changes from 0.01 to 11475 mD. In all regions, the number of data are large enough to make the statistics reliable. However, in region B, which is the largest dataset, we got the lowest correlation coefficient due to the dispersion of the data and even simple statistics show lack of homogeneity of samples. Although varying over a large range, porosity datasets are more compact than permeability datasets. So, arithmetic averages of porosity can well illustrate the means, all the more in most cases the geometric averages are close to the arithmetic ones. Permeability datasets cover the large ranges, especially in region B. The outliers occurring at either side of the range cause that the geometric averages were more reliable than the arithmetic ones. Both averages are included in Table 3, and the difference is high in almost all regions and groups with the exception of groups B3 (only one well WRZ-IG1) and B5 (wells KAZ-1 and OB-IG1), where we do not observe the outliers. This high variability of petrophysical parameters is caused by combination of diagenetic and compaction factors, which are very unstable across the study area (Biernacka *et al.*, 2006; Maliszewska *et al.*, in Górecki *et al.*, 2008). These

Table 2

Wells grouped in selected regions

No	Region/ group	Location	Nr of samples	Depth of top of the Rotliegend	Wells
1	A	vicinity of Kościan	221	2595 - 3710	PA-1, KA-1, GR-2, GO-1, S-2.
2	B/ B1-B6	neighbourhood of Kalisz and Sieradz	1298	2760 - 4889	B1-KOT-1, BR-1, KOW-1, LU-1; B2- KO-1, SM-1, W-1, KR-1A, W-1, SO-2, ME-3, PO-1, KA-4, KR-1; B3- WRZ-IG1; B4- SI-3; B5- KAZ-1 and OB-IG1; B6- KU GR-1 and ST-1
3	C	northwestern Poland	421	2940 - 3860	M-5, SLO-1, SLE-1, C-1, C-5
4	D	southern part of the Wolsztyn High within the Zielona Gora Trough	366	1363 - 2172	D-1, JE-1, SW-1, Z-1, CZE-3, GRA-1, WIE-1, BA-1, BO-1, BRO-2, ZA-6, CHW-1, KOC-1, WY WI-1

Table 3

Basic statistics for the data of grouped wells

Region/ group	Number of data	Equation: $\log K = a\Phi_{\text{eff}} + b$		$\Phi_{\text{eff}}^{\text{min}}$ [%]	$\Phi_{\text{eff}}^{\text{av}}$ [%]	$\Phi_{\text{eff}}^{\text{max}}$ [%]	K^{min} [mD]	$K^{\text{av}}/K^{\text{geom}}$ [mD]	K^{max} [mD]	Correlation coefficient R
		a	b							
A	221	0.18	-1.62	0.00	7.8	21.90	0.02	9.61/0.66	274.51	0.72
B	1298	0.10	-0.76	0.00	11.37	26.14	0.01	77.14/2.26	11475	0.46
B1	148	0.08	-1.08	3.73	15.93	26.14	0.01	34.41/1.03	470.63	0.32
B2	694	0.11	-0.56	0.11	11.77	23.99	0.01	102.78/5.5	11475	0.46
B3	87	0.06	-0.61	0.25	6.67	14.10	0.10	0.97/0.63	9.5	0.50
B4	247	0.05	-1.11	0.00	10.60	19.24	0.02	8.07/0.69	361.29	0.18
B5	94	0.07	-0.86	0.11	6.14	14.21	0.13	0.86/0.39	18	0.59
B6	28	0.10	-0.82	1.18	11.29	18.43	0.1	84.49/1.81	1874	0.39
C	433	0.19	-1.83	0.56	6.51	24.96	0.02	12.36/0.27	649.88	0.81
D	363	0.14	-1.52	0.00	12.3	26.00	0.02	11.77/1.80	540.11	0.68

results seem to be characteristic for the shallower part of the Rotliegend basin. High correlation coefficient of $R = 0.81$ is obtained for region C. The average effective porosity is 6.51 per cent while its maximum value is 24.96 per cent and minimum value is 0.56 per cent. The arithmetic average for permeability is at a level of 12.36 mD but the geometric mean equals to 0.27 mD. Region D has lower correlation coefficient, $R = 0.68$, and the average of effective porosity of 12.3 per cent and arithmetic average of permeability of 11.77 mD while geometric mean equals to 1.80 mD. Generally, in all regions and groups, porosity is quite high but permeability is rather medium, which indicates moderate reservoir parameters.

Dispersion plots for permeability vs. porosity for the whole region A and for individual wells are shown in Figure 5. Regression lines are similar in plots for individual wells and for the whole dataset. A similar presentation for the whole B2 group is shown in Figure 6. Great dispersion of data is observed in plot $\log K$ vs. Φ_{eff} . Except the W-1 well, concentration of points along regression lines can be clearly seen in the dispersion plots for datasets for individual wells (Fig. 6), although in a few cases the size of datasets is small.

High correlation coefficients are characteristic of all dependences in figures 5 and 6. In Figure 6 and in Table 3 we observe that the slopes of regression lines are variable, what can be attributed to different structure and texture and different mineral composition of sandstones in each well. From the analysis of the plots in figures 5 and 6 we can conclude that variability of sandstone samples in the group B2 is greater than in the region A.

Frequency histograms show close to normal porosity distribution and log-normal distribution of permeability for all regions and groups. Exemplary plots for region A are given in Figure 7. The log-normal character of permeability distribution shows the dominant contribution of samples with small permeability.

The presented analysis of distributions of porosity and permeability in individual wells and in regions or groups illustrated by the scatter of points in figures 3, 5 and 6 and data listed in Table 3 suggest that rather than permeability vs. porosity dependence, a more effective parameter or relation should be sought to describe the Rotliegend sandstone reservoir parameters.

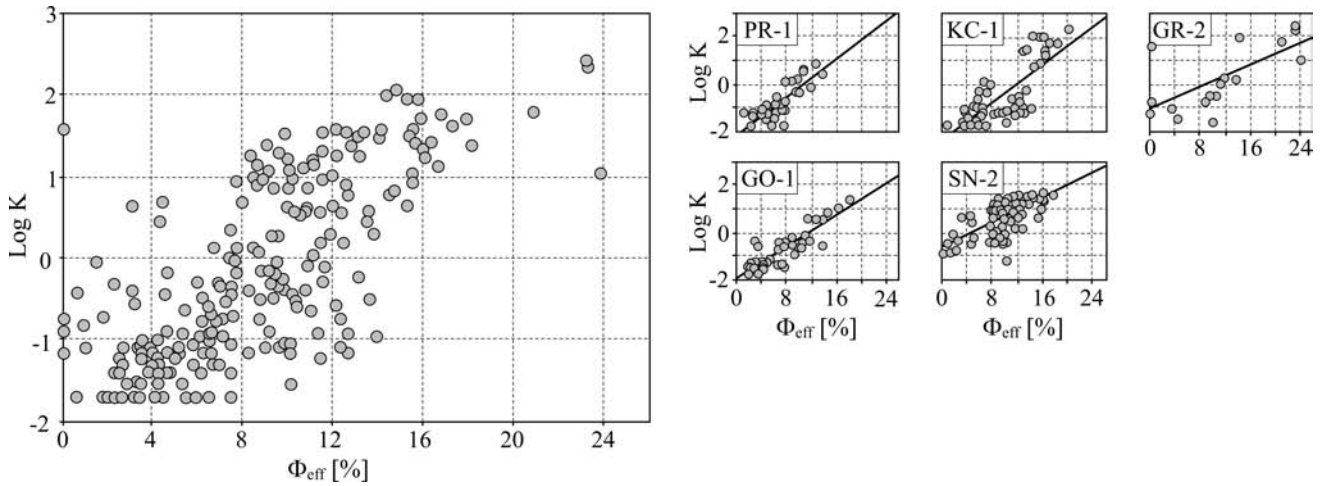


Fig. 5. Dispersion plots of $\log K$ vs. Φ_{eff} for data from the region A and for individual wells from region A

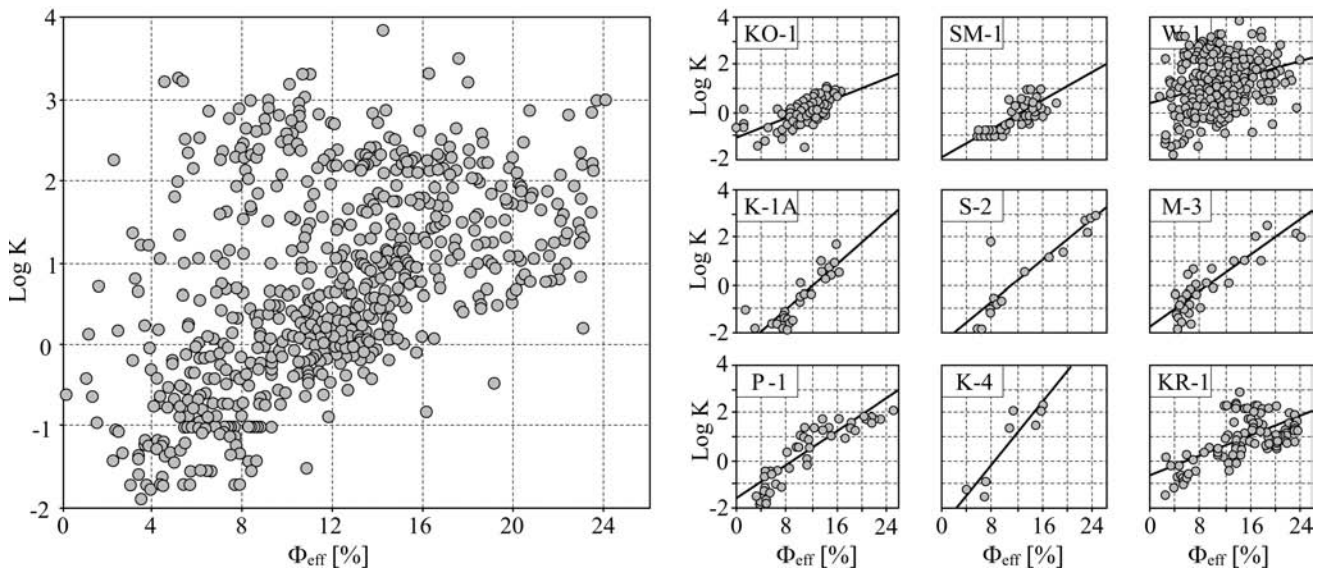


Fig. 6. Dispersion plots of $\log K$ vs. Φ_{eff} for data of group B and for individual wells from group B2

FLOW ZONE INDEX, FZI

To better divide the permeability-porosity area, the Flow Zone Index (FZI) was applied (Prasad, 2000; Tiab & Donaldson, 2000; Mohammed & Corbett, 2003). The FZI contains information on rock ability to transport fluid through its pore space and allows a series of deposits to be divided into smaller units with similar hydraulic capability. The FZI value was calculated from the following formula:

$$FZI = (A / \sqrt{\frac{K}{\Phi}}) / \left(\frac{\Phi}{1} \right);$$

where: K is permeability (mD), Φ is porosity, and A is a scale factor.

It is assumed that reservoir parameters in units with constant FZI undergo only small changes. In this analysis, the number of FZI classes was evaluated by means of the iteration method.

Plots $\log K$ vs. Φ_{eff} for region A are shown in Figure 8. Data from different wells are marked with different colours; data from units with given FZI are also presented with different colours. Eight FZI classes were distinguished for the region A. The highest value of FZI slightly surpasses 10.

Ten FZI classes were distinguished in the group B2 (Fig. 9). FZI values in the top class exceeded 100. Regression equations (fitting curves for each FZI) and corresponding correlation coefficients for the classes in region A and group B2 are given in Table 4. The correlation curves in figures 8 and 9 are parallel and slopes in the correlation equations are similar. Correlation coefficients calculated for individual FZI classes are higher than for single wells and regions or groups of datasets. High correlation coefficients obtained for the permeability vs. porosity relations in the individual classes with constant FZI prove that FZI ranges are correctly chosen. Better hydraulic properties resulting in enhanced fluid flow capability are observed with increasing

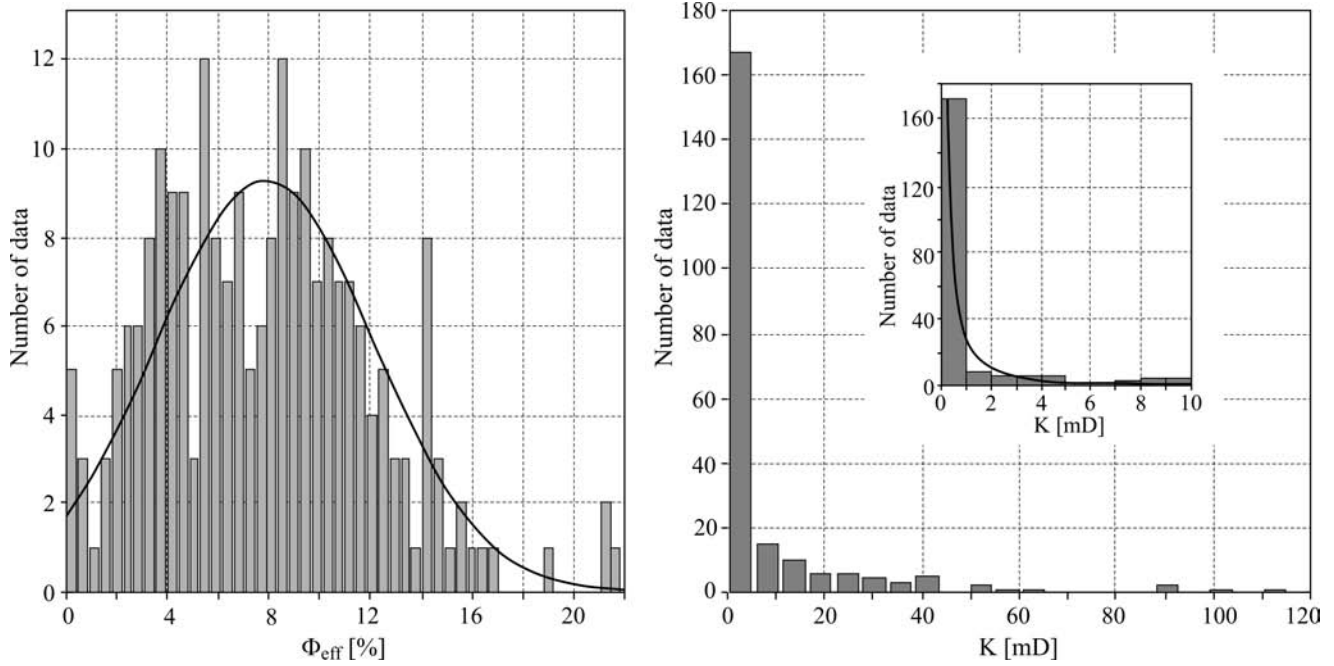


Fig. 7. Frequency histograms of effective porosity, Φ_{eff} , and permeability, K , for the data from the region A

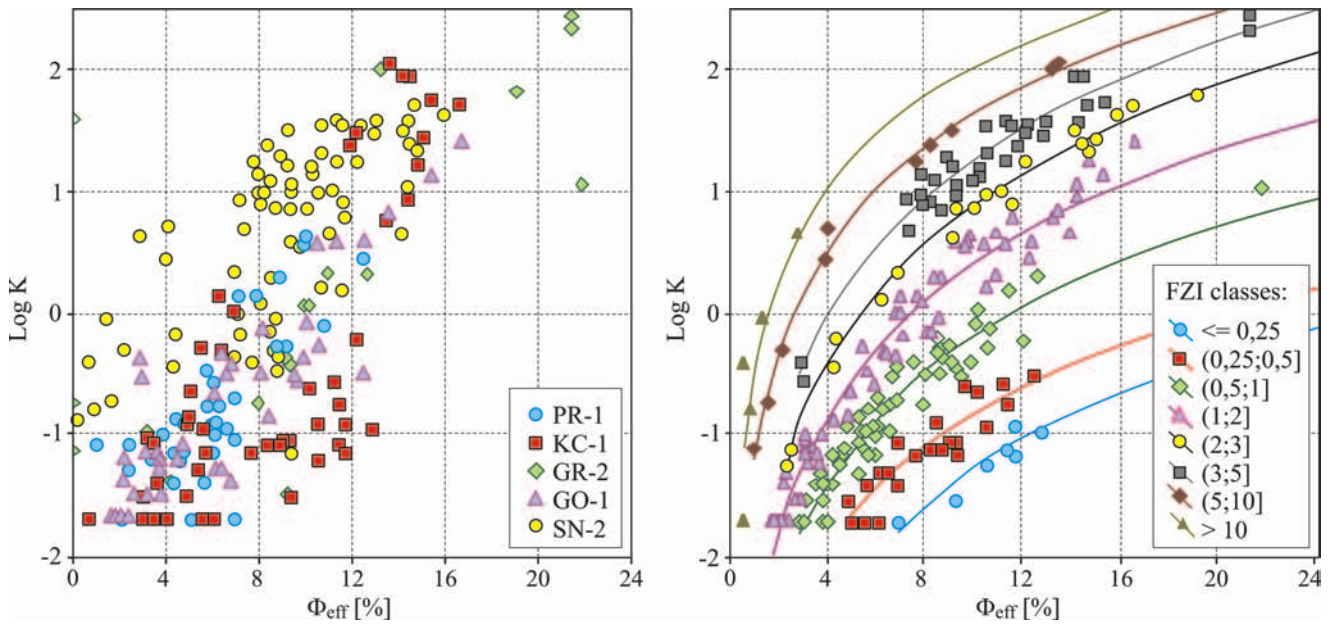


Fig. 8. Dispersion plots $\log K$ vs. Φ_{eff} in the region A: colours mark data from various wells (left) and data from units of constant FZI (right)

FZIs (Bała & Jarzyna, 2004). In the discussed cases most FZI values fall within the range 0.5–2.0. Certain outliers are observed for eight FZIs for W-1 well. Permeability measured there approaches the value of some 1000 mD.

Therefore, the calculated values of FZI are greater than 100, and the correlation curve with $FZI > 100$ differs from other curves. Great permeability results probably from the fractures. Some fractures are identified and described in some cores (Górecki *et al.*, 2008).

Similar studies were made for regions C and D. Eight FZI classes were revealed in region C while seven – in region D (Table 5). The FZI classes have the greatest number

of points in ranges (0.5;1) and (1;2). This reflects the moderate hydraulic properties of the studied sandstones.

It can be seen from the study that the analysis made for individual FZI classes gives more detailed dependences $\log K$ vs. Φ_{eff} with higher correlation coefficients. Using the FZI, the porosity–permeability area was divided into parts with the same hydraulic flow parameters. The enhancement of fluid flow capability is observed with increasing FZI. In the study area, we revealed a great number of units with good reservoir properties and good fluid flow capability, which were not identified earlier based on simple permeability vs. porosity relations.

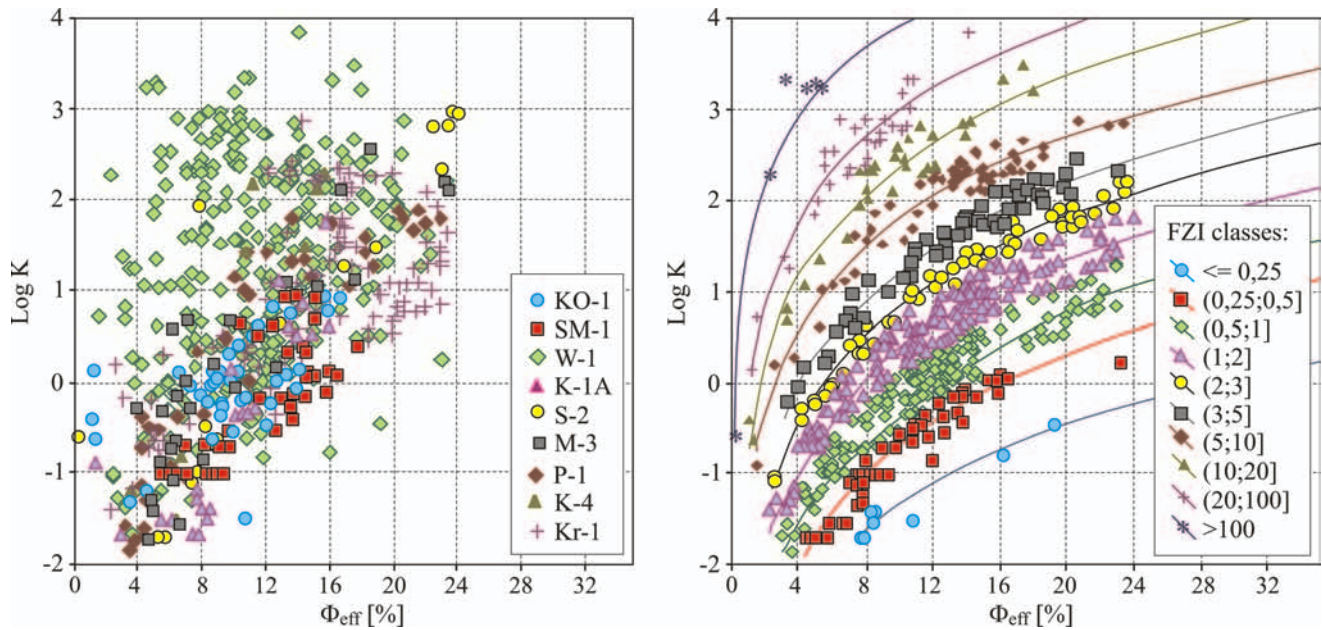


Fig. 9. Dispersion plots $\log K$ vs. Φ_{eff} in the group B2: colours mark data from various wells (left) and data from units of constant FZI (right)

Table 4

Regression equations for units of constant FZI for the region A and group B2

Range of FZI	Equation: $\log K = a\Phi_{\text{eff}} + b$		Number of data	Range of FZI	Equation: $\log K = a\Phi_{\text{eff}} + b$		Number of data
Region A				Group B2			
	a	b			a	b	
$\leq 0,25$	3.09	-4.39	8	0,25	2.80	-4.12	8
(0,25;0,5]	2.73	-3.55	22	(0,25;0,5]	3.32	-4.01	53
(0,5;1]	2.99	-3.18	62	(0,5;1]	3.21	-3.38	184
(1;2]	3.13	-2.72	59	(1;2]	3.20	-2.81	171
(2;3]	3.28	-2.39	21	(2;3]	3.25	-2.39	62
(3;5]	3.21	-1.95	34	(3;5]	3.22	-1.95	61
(5;10]	2.79	-1.15	10	(5;10]	3.06	-1.26	72
>10	2.48	-0.46	5	(10;20]	3.17	-0.75	37
				(20;100]	3.06	-0.06	34
				>100	2.31	1.60	8

DESCRIPTIVE STATISTICS

Basic statistical parameters of FZIs, i.e. means, medians, variances, and standard deviations are calculated for each region (Tab. 6). The largest mean value for FZI (11.74) is obtained for the group B2. Also, in region B the highest maximum FZI of 3904.21 is observed. The maximum values in other sets do not exceed 47. Extremely low value of median in comparison with the arithmetic average and very high maximum value confirms that there are many low values and the only one high extreme cannot balance the normal distribution. Such data distribution results in extremely high variance and standard deviation. Results from group B2 after excluding the highest outliers are presented in row

2* (Tab. 6), showing distinctly lower statistics. More variable FZI values are observed for region A and group B2 than for other regions (C and D). $FZI \in \langle 0.12; 17.17 \rangle$ for region C and $FZI \in \langle 0.09; 20.70 \rangle$ for region D. Both the mean $FZI = 1.95$ and more 'outlier-proof' median are higher for dataset C than for dataset D. Comparing the values of variance suggests that petrophysical parameters for both regions vary over a similar range, while the mean value of variance for dataset C is a bit higher.

Datasets in the regions A, C and D and group B2 include samples of various sandstones formed in diverse sedimentation environments. According to facies distribution (Figs 1, 5) region A includes wells sited in the area of domination of aeolian facies and fluvial facies. Wells from group

Table 5

Regression equations for units of constant FZI for the regions C and D

FZI	Regression equation: $\log K = a\Phi_{\text{eff}} + b$		Number of data	FZI	Regression equation: $\log K = a\Phi_{\text{eff}} + b$		Number of data
Region C				Region D			
	a	b			a	b	
0.25	1.39	-4.65	9	0.25	1.16	-4.02	35
(0,25;0,5]	1.17	-3.52	64	(0,25;0,5]	1.37	-3.91	51
(0,5;1]	1.35	-3.32	120	(0,5;1]	1.34	-3.25	113
(1;2]	1.37	-2.75	110	(1;2]	1.41	-2.85	93
(2;3]	1.39	2.29	40	(2;3]	1.37	-2.27	42
(3;5]	1.36	-1.88	47	(3;5]	1.32	-1.84	21
(5;10]	1.3	-1.27	22	>5	1.16	-0.74	11
> 10	1.33	-0.68	9				

Table 6

Basic statistics of FZI in the regions A, C and D and group B2

No.	Region/group	Number of data	Mean	Median	Minimum	Maximum	Variance	Standard Deviation
1	A	221	2.25	1.24	0.17	46.53	14.61	3.82
2	B2	694	11.74	1.46	0.15	3904.21	22559.62	150.20
2*	B2*	690	5.45	1.45	0.15	438.38	397.54	19.94
3	C	421	1.95	1.13	0.12	17.17	6.16	2.48
4	D	365	1.46	0.93	0.09	20.70	4.24	2.06

B2 belong to aeolian facies. Wells from region C are situated in fluvial facies area with the exception of well M-5, which is sited in the area of aeolian facies. Region D covers the area of aeolian facies, but in the centre of it wells SW-1 and Z-1 belong to the playa facies. Also, in the whole region D an admixture of fluvial sediments is observed. Additionally, discussing the variability of data one should take into account the shaliness of sediments. Almost all sandstones in the Rotliegend sediments are shaly, but the volume and type of clay minerals are variable. In region A and group B2, illite domination is noted. However, region C with very similar FZI characteristic to region A comprises samples where kaolinite and chlorite are most frequent. Region D covers an area of the greatest amount of illite. The Rotliegend sandstones are also diverse as regards to the type of nonclay cement (Maliszewska *et al.*, in Górecki *et al.*, 2008). In sandstones from region A, for instance in well PR-1, we can meet even 37 per cent of matrix, while in region C only a few per cent and in region D – a dozen or so. In region B matrix cement is at the level of several per cent, while in well SI-3 it amounts to 24 per cent. Numbers shown in Table 6 and in the previous ones illustrate the variability of features of sandstones belonging to the Rotliegend.

Petrophysical information on sandstone samples from these datasets explains the differences. To compare selected samples from regions A and C of $FZI \in (0.5; 2)$, *i.e.* the most frequent in all analysed datasets, histograms of effective porosity, Φ_{eff} , and permeability, $\log K$, and FZI are presented (Figs 10 and 11). Distributions closer to Gaussian are observed in comparison with the previously mentioned histograms. It means that more homogeneous parts of sandstone

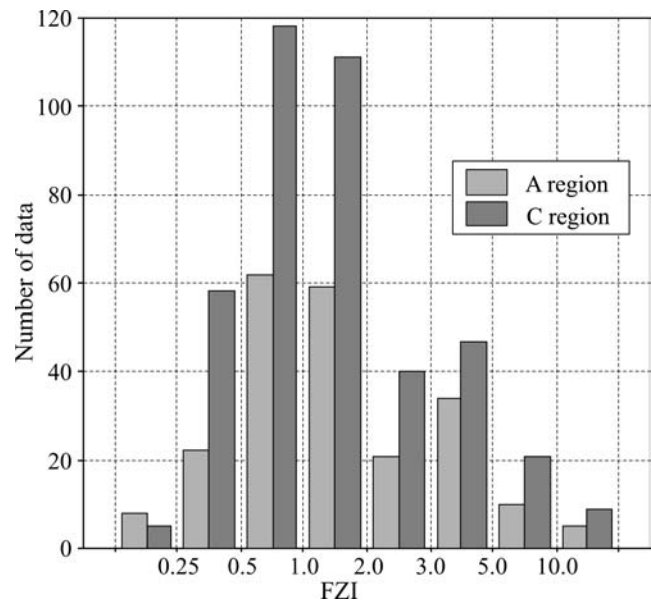


Fig. 10. Comparison of histograms of FZI in the regions A and C

osity, Φ_{eff} , and permeability, $\log K$, and FZI are presented (Figs 10 and 11). Distributions closer to Gaussian are observed in comparison with the previously mentioned histograms. It means that more homogeneous parts of sandstone

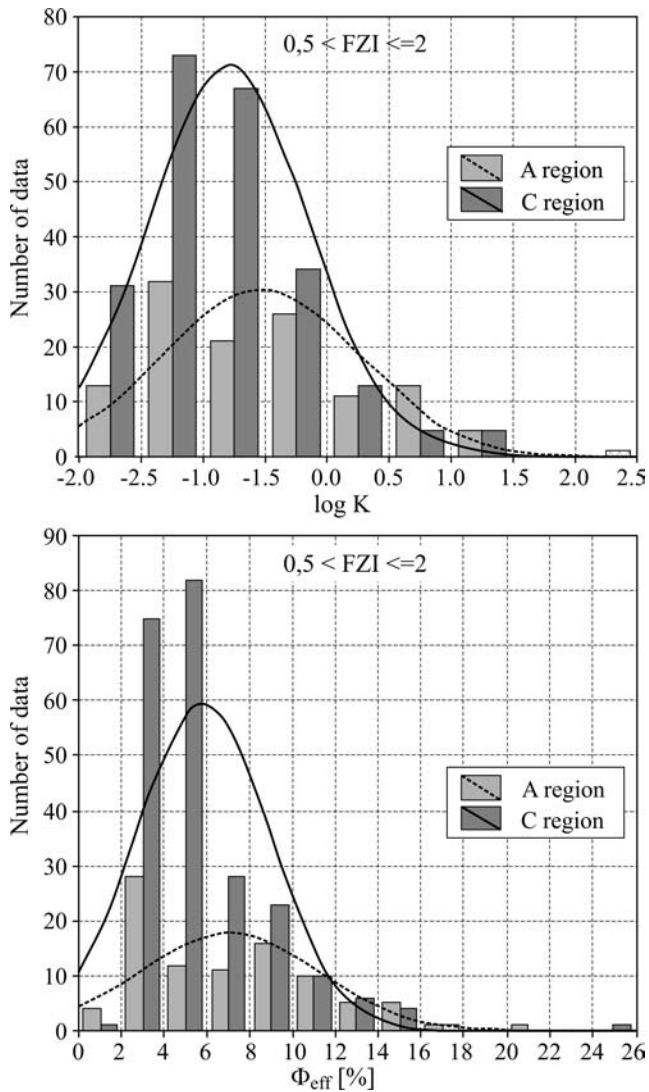


Fig. 11. Frequency histograms of porosity and permeability for samples of the region A and region C

samples were clustered due to FZI classification. The analysis of the basic statistics for the data from regions A and C, in FZI range of (0.5–2] confirms the conclusion that FZI classes gathered data of great similarity (Tab. 7).

FZI DEPENDENCE UPON FACIES DEVELOPMENT

Information on the facies development is available only from a limited number of samples: from single wells of the region A, C and D and from five wells of the group B2. Facies identification in individual wells in the group B2 is not uniform; therefore besides the undivided aeolian facies we observe also aeolian dune and aeolian interdune ones and in the other regions not separated fluvial/alluvial fan facies. Means, medians, minimal and maximal values, and standard deviations of FZI for each facies are listed in Table 8. The highest FZI values are observed for the undivided aeolian facies in group B2: the highest arithmetic mean of 12.08 and the median of 0.90 causes calculation of the geometric mean of 1.77 more justified in dataset with outliers. A number of samples with FZI greater than 20 and several outliers reaching the value of 3904.21 were observed for the undivided aeolian facies of the group B2. Generally, undivided aeolian facies datasets include high maximum values. Similarly, high values of FZI were observed for the fluvial facies: the maximum value was 127.69 and the mean and median were 8.67 and 2.34, respectively. Such results can be explained on the basis of great variability of sandstone samples and not completely proper classification to facies. The lowest values of FZI are characteristic of the playa facies and alluvial fan facies.

The number of data in facies classes is also of great importance. The most reliable results are those in classes of the largest number of data, *i.e.* aeolian dune facies in group B2 ($N = 296$) and fluvial/alluvial fan facies in region D ($N = 186$) and C ($N = 83$). Worth of discussion are especially results for the fluvial/alluvial fan facies, where we do not observe large variability of data in region C (standard deviation are equal to 0.65) and one of the greatest standard deviation 3.17 for region D. Minimum values of FZI in the discussed datasets are not very diverse, *i.e.* 0.14 for the fluvial facies and 0.51 for the alluvial fan facies in region D, what means that low FZI are met everywhere. Standard deviation as a measure of dispersion of data covers a big range, from 0.27 for the playa facies in region D to 45.46 for the undivided aeolian facies in group B2, skipping the value of 0.11 for the alluvial fan facies in region C due to the small number of data.

Table 7

Basic statistics for porosity and permeability of samples of FZI from the range (0.5 – 2] for the region A and region C

	Region	N	Mean arithmetic	Mean geometric	Min	Max	Variance	Standard deviation
Φ_{eff}	A	121	7.04	6.14	1.73	21.90	13.60	3.69
K			1.50	0.28	0.02	24.89	12.14	3.48
Φ_{eff}	C	229	5.80	5.20	1.86	24.96	9.61	3.10
K			1.15	0.16	0.02	104.66	52.60	7.25

Table 8

Basic statistics of FZI for the facies development in the regions A, C and D and group B2

Region/group	Facies	FZI					
		N	Mean	Median	Standard deviation	Minimum	Maximum
A	Undivided Eolian	50	2.33	1.19	3.08	0.19	18.63
	Fluvial	53	3.99	2.80	6.58	0.31	46.53
	Alluvial fan	47	1.25	0.94	1.56	0.17	10.83
B2	Undivided Eolian	111	12.08/1.77	0.90	45.46	0.32	438.38
	Aeolian Dune	296	3.83	1.69	5.85	0.15	42.30
	Aeolian Interdune	23	1.82	0.79	2.32	0.18	8.59
	Fluvial	99	8.67	2.34	16.17	0.32	127.69
	Alluvial fan	26	1.36	1.11	0.92	0.30	3.90
C	Undivided Eolian	28	2.06	1.76	2.56	0.19	12.56
	Fluvial	39	0.75	0.65	0.43	0.19	2.74
	Alluvial fan	4	0.56	0.51	0.11	0.48	0.72
	Fluvial/Alluvial fan	83	1.29	1.13	0.65	0.34	3.89
D	Undivided Eolian	83	1.10	0.75	1.04	0.26	5.31
	Fluvial	81	2.20	1.53	1.94	0.14	12.40
	Fluvial/Alluvial fan	186	2.55	1.55	3.17	0.17	17.17
	Alluvial fan	18	2.76	1.52	2.30	0.51	7.39
	Playa	41	0.60	0.56	0.27	0.25	1.77

PERMEABILITY PREDICTION FROM WELL LOGS ON THE BASIS OF STATISTICAL MODELS FROM LABORATORY DATA

Porosity, PHI, from the comprehensive interpretation of well logs was correlated with laboratory-determined porosity, Φ_{eff} . The following factors, which required great caution in connecting the both datasets, were regarded:

- samples for laboratory tests have small size and therefore give pointwise information; samples are usually cut out of most compact core fragments and hence provide information only on that part of rock,

- neutron, acoustic, and density logs are used to evaluate the lithology and porosity; information about a rock medium delivered by those logs depends on vertical resolution and radius of investigation of a probe; it can be taken that information is gathered from a zone around a well with the radius of 0.30 to 0.50 m.

Moreover, we observe relatively low correlation coefficients due to the depth shift in correlated data.

Because of the large number of available laboratory data and identified facies, the dependence of PHI vs. Φ_{eff} was made for the W-1 well (the group B2, eolian facies area) over the interval of the Rotliegend sandstones. 349 samples were obtained from 11 intervals (from 3370 to 3960 m). In each depth interval 13 to 65 samples were grouped in 0.5 m sequences.

First, the mineral composition determined from the comprehensive interpretation of logs was analysed. It is found that in addition to sandstone volume, shales and admixture of carbonates are present in the Rotliegend rocks. The shale volume ranges from a few to over 60 per cent. At $V_{\text{SH}} > 40$ per cent, the effect of shale volume on the interpreted porosity, PHI, was substantial and therefore it was decided to eliminate intervals with high shaliness from the

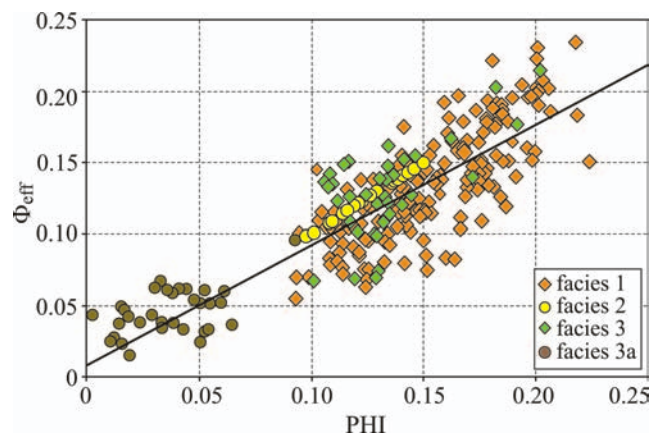


Fig. 12. Dispersion plot Φ_{eff} vs. PHI; facies marked with colors: dune (1), interdune (2), fluvial sandstone (3) and fluvial shaly sandstone (3a) from the depth interval 3,945.1–3,960.0 m

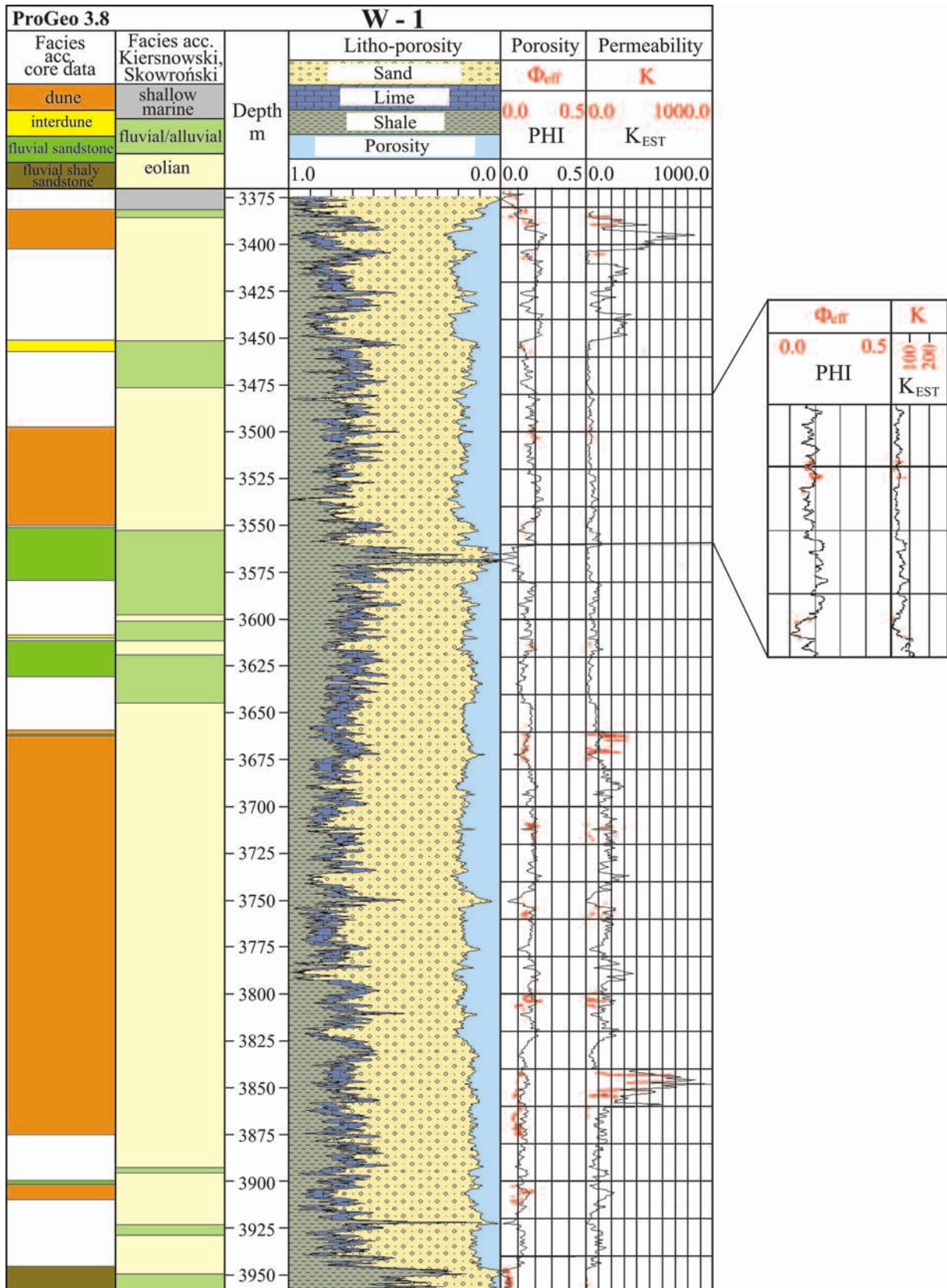


Fig. 13. Results of the permeability prediction on the basis of FZI definition for sediments of various facies in W-1 well

datasets. While tying laboratory data, Φ_{eff} , to PHI, we removed fractured samples and the data of which the permeability, K , was a few hundred mD at minimum porosity (5 points corresponding to undivided aeolian facies). For the dataset of 229 observations, we obtained the coefficient of determination, $R^2 = 0.76$, which evidences that some 86 per cent of variability was explained in the regression (Fig. 12). Different colours are used to mark samples belonging to the dune aeolian facies (1), interdune facies (2), fluvial sandstone facies (3), and fluvial shaly sandstone facies with much increased shaliness (3a); the latter is corresponding to the interval of 3,945 to 3,965 m. Although there is a distinct scatter of points, the observations belonging to different facies cover similar variability areas.

High determination coefficient justifies the permeability prediction, K_{EST} , with the use of the obtained regression equations, K vs. Φ_{eff} , in the FZI classes. Equations given in Table 4 for the group B2 were used to estimate K_{EST} . The variable Φ_{eff} was substituted with $\Phi_{\text{eff-corr}}$, which was correlated with PHI based on the regression equation (Fig. 12). Assuming mean FZI values for each depth interval corresponding to different facies, we obtained K_{EST} for sandstone intervals (Fig. 13). Porosities obtained from lab data and well logs (track 3) and permeability: estimated, K_{EST} , and laboratory-based, K , (track 4) are shown together with mineral components and porosities interpreted from well logs (track 2). The agreement between the results is satisfactory; however in some intervals one can observe discrepancies. It seems likely that substantial differences in laboratory-based values of permeability observed for samples drawn near one another from sandstone intervals can evidence the occurrence of fractures and micro-heterogeneities in cores that could not be visible in well logs. The continuous calculation of rock permeability, K_{EST} , based on statistical models, gives additional information that is independent of results obtained from formulae by Kozeny–Carman or Timur, routinely used in world interpretation systems or the formula by Zawisza used in Polish interpretation (Zawisza *et al.* 1995). Porosity and permeability correlate with facies distribution (Fig. 13). Two facies columns correspond to results of H. Kiersnowski L. Skowroński and to core description (Górecki *et al.*, 2008). High reservoir parameters correspond to aeolian facies. Dune facies section is of highest values of porosity and permeability. Fluvial/alluvial fan sections show distinctly lower values. The lowest porosity and permeability occur in fluvial shaly sandstone section.

CONCLUSIONS

1. Relationships between porosity and permeability in classes with constant fluid transport parameters determined based on FZI are more exact than the same relationship for the whole dataset.
2. In all studied datasets of the Rotliegend sandstones, the largest FZI classes belong to ranges (0.5;1] and (1;2]. Rocks with those FZIs have moderate reservoir parameters.
3. The sporadically occurring extremely high FZI (>100) are related to samples with cracks in identified cores.
4. FZI takes the highest values for aeolian and fluvial

facies, while the smallest values were observed for the playa facies and alluvial fan facies.

5. Clustering sandstone samples according to FZI in selected facies area makes datasets more homogeneous.

6. Using the derived statistical relations K vs. Φ_{eff} for various FZI and substituting Φ_{eff} with PHI interpreted from well logs allows the permeability of the Rotliegend section to be calculated for each facies in a continuous way.

Acknowledgements

Authors thank the Polish Oil and Gas Company, Warsaw, Poland to make available laboratory data and well logs and to the Ministry of Environment of Poland to allow to publish the results obtained partly during the realization of the project nr 562/2005/Wn-06 /FG-sm-tx/D. Authors also thank Mr. Arkadiusz Buniak (POGC, Zielona Góra / Piła Branch) for the discussion and Prof. Dr. Anna Maliszewska, Polish Geological Institute, Warsaw, for the information about cements of the Rotliegend sandstones. Authors thank the Reviewers, Mr. Hubert Kiersnowski from the Polish Geological Institute, Warsaw, and an Anonymous Reviewer. Special thanks are due to Prof. Dr. Jan Golonka – Editor, for his friendly help in making the matter more clear and understandable for readers.

REFERENCES

- Attia, A., M., 2005. Effects of Petrophysical Rock Properties on Tortuosity Factor. *Journal of Petroleum Science and Engineering*, 48: 185–198.
- Bała, M. & Jarzyna, J., 2004. Relationship between porosity and permeability in reservoir rocks using the factor characterizing pore space. (In Polish, English summary). *Proceedings of Geopetrol 2004, Prace Instytutu Nafty i Gazu, Cracow, Poland*, 130: 275–277.
- Bała, M., Jarzyna, J. & Cichy, A., 2003. *Modeling of velocity and attenuation of elastic compressional and shear waves in porous rocks using well logging data*. (In Polish). Report of scientific project no 8 T12B 046 20 financed by Polish Committee of Scientific Research. Department of Geophysics, Faculty of Geology Geophysics and Environmental Protection, AGH UST, pp. 98.
- Biernacka, J., Leśniak, G. & Buniak, A., 2006. Compaction versus cementation influence on reservoir properties of Rotliegend aeolian sandstones, Fore-Sudetic Monocline, SW Poland. (In Polish, English summary). *Prace Instytutu Nafty i Gazu, Cracow, Poland*, 134: 67 pp.
- Górecki, W., Papiernik, B., Bała, M., Jarzyna, J., Krawiec, J. & Puskarczyk, E., 2008. *Prognostic resources and undiscovered natural gas-potential of Rotliegend and Zechstein limestone deposits in Poland*. (In Polish). Report of the project no. 562/2005/Wn-06/FG-sm-tx/D funded by Ministry of Environment of Poland in 2005–2008. pp. 196. Department of Fossil Fuels, Faculty of Geology Geophysics and Environmental Protection, AGH UST.
- Jarzyna, J. & Bała, M., 2005. Relationships between petrophysical parameters of the Carboniferous clastic rocks in the Steżyca hydrocarbon deposit, Lublin Basin. (In Polish, English summary). *Kwartalnik AGH, Geologia*. 31: 337–355.
- Karnkowski, P.H., 1987. Lithostratigraphy of the Rotliegend in Wielkopolska (Western Poland). *Geological Quarterly*, 31: 643–672.
- Kiersnowski, H., 1997. Depositional development of the Polish

- Upper Rotliegend Basin and evolution of its sediment source areas. *Geological Quarterly*, 41: 433–456.
- Kiersnowski, H., 1998. Depositional architecture of the Rotliegend basin in Poland. (In Polish, English summary). *Prace Państwowego Instytutu Geologicznego*, 165: 113–128.
- Kiersnowski, H. & Buniak, A., 2006. Evolution of the Rotliegend Basin of northwestern Poland. *Geological Quarterly*, 50: 119–138.
- Mohammed, K. & Corbett, P., 2003. How many relative permeability measurements do you need? A case story from North African reservoir. *Petrophysics*, 44: 262–270.
- Papiernik, B., Protas, A., Semyrka, R. & Zając, A., 2007. *Diagenetic processes versus reservoir properties of Rotliegend sandstones in: The new strategy and perspectives of natural gas fields exploration in Rotliegend deposits*. (In Polish, English summary). Project financed by the Committee of Scientific Research of Poland, no 6 T12 2003C/06292. pp 194. Department of Fossil Fuels Faculty of Geology Geophysics and Environmental Protection, AGH UST.
- Pokorski, J., 1981. Formal lithostratigraphic subdivision proposed for the Rotliegend of the Polish Lowlands. *Geological Quarterly*, 25: 41–58.
- Pokorski, J., 1997. The Lower Permian (Rotliegend). (In Polish, English summary). *Prace Państwowego Instytutu Geologicznego*, 153: 35–62.
- Pokorski, J., 1998. Prospects of the occurrence of gaseous hydrocarbons in the Rotliegend deposits. (In Polish, English summary). *Prace Państwowego Instytutu Geologicznego*, 165: 293–298.
- Poszytek, A., 2007. Sedimentary Processes Diversifying Reservoir Properties of the Upper Rotliegend Deposits in the Fore-Sudetic Monocline. *Proceedings of the 69th Conference and Exhibition of EAGE & SEG, P133, London, 11–14th June 2007*, pp. 4.
- Prasad, M., 2000. Velocity-permeability relations with hydraulic units. *Geophysics*, 68: 108–117.
- Salem, H. & S., 1993. Derivation of the cementation factor (Archie's exponents) and Kozeny–Carman constant from well log data and dependence on lithology and other physical parameters. *SPE Paper*, V. 26309.
- Tiab, D. & Donaldson, E., C., 2000. *Petrophysics, Theory and Practice of Measuring Reservoir Rock and Fluid Transport Properties*. (2nd Edition), Elsevier, N.Y., 899 pp.
- Zawisza, L., Gądek, W., Nowak, J. & Twaróg, W., 1995. Estimation of permeabilities and irreducible water saturation for sandstone-clay formations from well logs. *Book of Abstracts of Conference and Exhibition "Modern Exploration and Improved Oil and Gas Recovery Methods"*. PB-04. 194–196.